Original Research Article

Modeling and Optimization of Photocatalytic Degradation of Methylene Blue via TiO_2-CuO/HApCatalyst: The Use of Response Surface Methodology and Artificial Neural Network

Abstract

This study is focused on the evaluation of the photocatalytic activity of TiO_2-CuO/HApcatalyst as prepared by sol-gel method and characterizedusing FT-IR, XRD, SEM-EDX for the degradation of Methylene Blue (MB) from its aqueous solution under sunlight. The effects of MB concentration,contact time, and catalyst dosage on the degradation of MB were studied using the central composite design (CCD) method.The Response Surface Methodology (RSM) and Artificial Neural Network (ANN) modeling techniques were also applied to model the process and examine their corresponding predictive and performance capabilities of the response (degradation efficiency).

The RSM optimized conditionsshow that TiO_2-CuO/HAp achieved 99.62% MB degradation in the designed photocatalytic system that was set under sunlight at 20 mg/L methylene blue concentration, 0.15 g TiO_2-CuO/HAp dosage and2.5hours (150mins) irradiation time. On the other hand, optimization with ANN study revealed that the predicated model was perfectly fitted with the experimental data.The process was also modeled using the adsorption isotherms and kinetic models.The degradation of MB was best described well by the Pseudo-Second-Order model with (R^2=0.995) and the equilibrium data for the photodegradation process fits well with the Langmuir isotherm model (R^2=0.996). The results ofour study will help communicate the most effective and economical options for the removal of dyes in wastewater

Keywords:*Artificial Neural Network, Isotherms, Kinetics, Photodegradation of Methylene Blue, Response Surface Methodology, TiO_2-CuO/HAp Catalyst*

1. Introduction

Dye effluents, especially synthetic dyes discharged from many dye-utilizing industries are harmful to the environment and living things at large[1]. It has been estimated that of about 100,000 commercially available dyes, 700, 000 tonnes of these coloring compounds are manufactured annually [2-3]. The continuous release of these untreated effluents from industries such as the textile, paper, leather, plastics, as well as pharmaceutical industries into environmental water bodies,is becominga growing concern to environmentalists and the ecosystem at large[4].A quite good number of these water-soluble organic substances, dyes,heavy metals, pharmaceutical products, pesticides e.t.c contaminate the water bodies or the environment they are being discharged, and the report reveals that the dye effluents released from many of these dye-utilizing industries are quite large and usually result into a significant environmental issue [3,4]. In particular, the textile industry among other dye-utilizing industries is said toutilize the highest number of dyes at approximately 10,000 tonnesper year globally[3,5].Methylene blue is a typical cationic dyewith a complex aromatic structure that has been in use for many years by several industries, though not regarded as acutely toxic but can have various harmful effects on human beings and as well as aquatic animals, especially on inhalation, it can give rise to short time difficulty in breathing while ingestion through the mouth can cause a burning sensation, nausea or vomiting [2]. Thus, the removal of dyes from aqueous effluents is necessary and itconstitutes one of the most significant efforts by the environmentalist. In addition, the wastewater treatment uses several methods for dyes elimination including physical (e.g adsorption, membrane separation, coagulation-flocculation, ion exchange e.t.c), Chemical (e.g ozonation, advanced oxidation process, Fenton reagent e.t.c) biological (e.g aerobic and anaerobic degradation processes, bacterial and fungal biosorption, algae e.t.c) and electrochemical

methods [6-8]. However, despite the current efforts with these methods, they are still unable to completely remove methylene blue compounds and some other dissolved organic contaminants in wastewater because some low biodegradable compounds remain resistant to these conventional elimination techniques [9].Hence, it is important to develop affordable alternatives and more cost-effective methods.

Currently, the photocatalytic degradation of pollutants in aqueous solutions using a light source is a more potentialtechnique owing to its high efficiency, economical, non-toxicity, and eco-friendly process [9-11].In the last few decades, heterogeneousphotocatalysis with different semiconductor (SC) oxides (e.g., TiO_2, ZnO, Fe_2O_3, SrO_2, WO_3, CeO_2, ZrO_2,etc.) has been an object of interest in the field of industrialwastewater treatment [12]. The principle is based on the formationof reactive species which are the photo holes (h+) and/or hydroxyl radicals (OH) upon the irradiation of the semiconductor oxide with a photon source (hv) higher than the band gap energy of SC oxide.The generated reactive species can undergo complete mineralization of the organic pollutants (e.g. dyes) into $CO_2$and H_2O [13]. Therefore, the anatase form of TiO_2 was found to be one of the most used photoactive SC oxides owing to its low cost, safety, photochemical activity, and stability [12,14].

Nevertheless, due to its bandgap, the photocatalytic activity of TiO_2 could be further enhanced by doping it with heteroatoms such as (N, C, S), transition metals (Fe, Co, V, Cr, Ni) and recently by the formation of heterojunctions between anatase TiO_2 and a semiconductor oxide with smaller band gap energy such as (CuO, WO_3e.t.c) which can act as a sensitizer [12].Thus,TiO_2 anatase is an *n*-type semiconductor with a larger band gap energy of 3.2 eV while CuO is a *p*-type semiconductor having a narrow band gap energy of 1.2 eV. A mixture of such semiconductor oxides exhibits good photocatalytic activity due to *p–n* heterojunctions that limit the recombination of charge carriers [12,15]. Hence, this present study reports the preparation of$CuO–TiO_2$-supportedhydroxylapatite composites developed as catalyst by sol–gel method for the degradation of methylene blue.

In past studies, the artificial neural network (ANN) has been used in various designs in the science and engineering fields and has given promising results as regards the prediction of output variables due to the use of approximation function to map complex nonlinear data[9]. ANN has also been used to remediate many environmental issues which include the degradation of pollutants[16].

In this present study, two different modelling and optimization systems which are RSM and ANN methods were used to optimize the methylene blue degradation process parameters and to establish a predictive model comprising three independent variables. The optimized parameters are methylene blue concentration, catalyst dosage, and irradiation time. These parameters will further be used for kinetic, equilibrium, and thermodynamic analysis studies. Different kinetic and isotherm models were applied to fitthe experimental data while thermodynamic analysis was also used to predict the nature of the photodegradation process of methylene blue.

2. Materials and methods

2.1. Chemicals and Reagents

Methylene blue (Sigma Aldrich) with the chemical formula $C_{16}H_{18}ClN_3S.3H_2O$ and its molecular weight of 319.86 $gmol^{-1}$ (the analysis done at wavelength 664 nm; Fig.1shows the chemical structure)Titanium dioxide (TiO_2) nanoparticles (purity ≥ 99.5%),$CuSO_4.5H_2O$(purity≥99%),NaOH(purity=98%), Na_2CO_3(purity=98%) and HCl (purity = 95%), Acetone(purity ≥ 95%)were used for the degradation studies. All chemicals are analytical grade and were used in the pure form as received with no further purification.

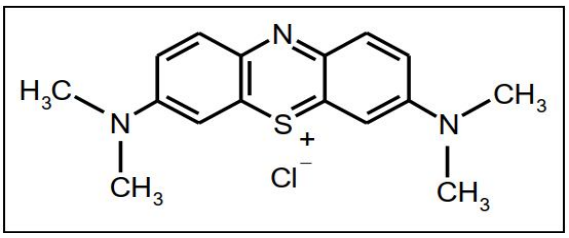

Fig. 1. Chemical structure of methylene blue

2.2. Catalyst Preparation

2.2.1 Synthesis of Hydroxylapatite powder

Firstly, the bovine bones were boiled in water for 1 hour to ensure deproteinization and easier removal of macroscopic adhering impurities. Afterward, the bones were washed and cleaned well with water to remove all the attached meat, bone marrows, tendons, and other soft tissues. The bones were then immersed in acetone for one hour and thereafter washed with water several times and dried to evaporate the absorbed water.

Furthermore, the dried bovine bones were carbonized at 400^0C for 1 hour and then crushed into small pieces using a mortar pestle and thereafter milled into smallerparticle sizes using the rotary mill. The bovine bones were sieved using 100µm mesh size to ensure uniform particle size.Finally, the sieved bovine was calcined at 900^0C for 2 hoursto obtain a white color powder ofnatural Hydroxyapatite.

2.2.2 Synthesis of TiO_2–CuO/HAp Composites

The preparation of TiO_2–CuOsupported Hydroxyapatite was done by a modified sol–gel method; 2.5g of Titanium dioxide (TiO_2) and 2.0g of Copper Sulphate Pentahydrate ($CuSO_4.5H_2O$) was dissolved separately each with 25ml of deionized water and later stirred together for 30 minutes. Thereafter, 1g ofhydroxyapatite (HAp) was added and stirred continuously with a magnetic stirrer at 300rpm, 80^0C for 1hr. A measured amount of 0.25M of Sodium Carbonate solution was also added dropwise to adjust the pH of the solution to 10. The dark grey precipitate was filtered, washed with deionized water, and dried at 80^0C for 4 hours. Finally, the dried catalyst sample was calcined at 400^0C for 3 hrs.

2.3. Photocatalytic degradation studies

The photocatalytic activity of the as-synthesized samples was investigated through the photocatalytic degradation of methylene blue(MB)under solar light irradiation between the hours of 10:00 am and 3:00 pm. For each batch photodegradation experiment, the degradation of methylene blue was carried out considering degradation factors such asinitial dye concentrations(5 to 35mg/L),catalyst dosage(0.05g to 0.25g), and Irradiation time(1 to 4 hours)using50 ml of the MB solution. Meanwhile, the pH of the prepared solutions was adjusted and maintained at 8 by using aqueous solutions of 0.1M NaOH and 0.1M HCl at room temperature[17].The desired parameter quantities were set, and the solution was continuously stirred for 60 min under dark conditions to attainan adsorption-desorption state before beingunder sunlight with continuous stirring usinga magnetic stirrer as shown in Figure 2.After the degradation experiment, 5ml of the degraded MB solution was withdrawn at different time intervals and centrifuged to remove the catalyst whilethe residual MB concentrations were analyzed using UV–Vis Spectrophotometer at λmax =664 nm.The MB degradationwas estimated through the following Eq. (1):

$$MB\ degradation\ efficiency = \frac{Co-Cf}{C} X\ 100 (1)$$

Furthermore,the amount of MB adsorbed on TiO_2-CuO/HAp catalyst, qe was obtained using Eq. 2 as follows.

$$qe = \frac{(Co-Ce)V}{M} \quad (2)$$

Where Co and $C_f$refer to initial and final concentrations of methylene blue at the time (t), Ce is the equilibrium concentration of MB (mg/L), V is the volume of the solution (L) and M is the amount of catalyst used (g).

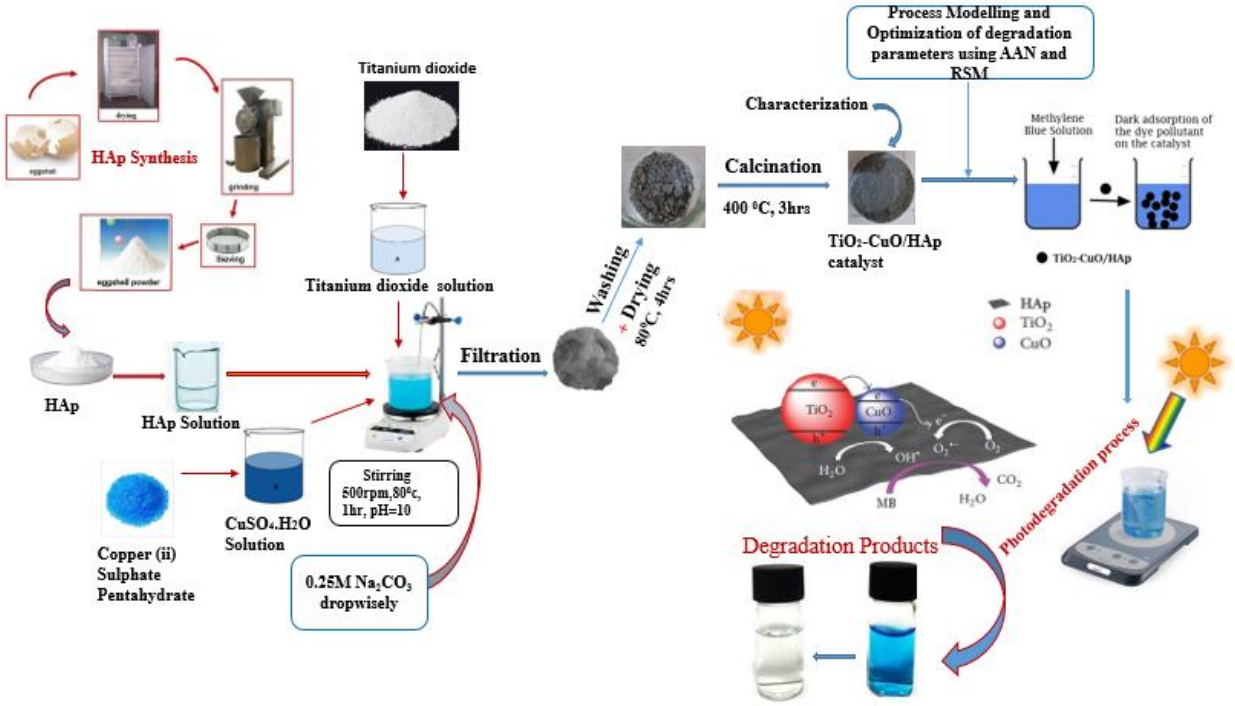

Fig. 2: The synthesis and Photocatalytic process of *TiO_2–CuO/HAp Catalyst*

2.4. Experimental design by RSM method

Response Surface Methodology (RSM) involves the use of statistical and mathematical approachesto analyze the importance of different process variables. DesignExpert Software (DES) (v12.0) was used to analyze the response of different independent parameters.

To optimize the operating conditions for maximum methylene blue degradation performance. Three independent factors including (i) MB concentration (ii) Catalyst dosage and (iii) Irradiation timewere fixed. The design is composed of three levels: low level or minimum (referred to as -1), centralreferred to as 0, and high level or maximum (referred to as +1) for all experimental variables.Table 1shows the operating levels andindependent variables evaluated in the study while Table 2shows the 20 experimental runs generated using CCD of RSM.These 3independent factors were represented as A, B,and C for MB concentration, Catalyst dosage, and Irradiation timerespectively.

The response, which is the degradation efficiency from the influence of each process variable,was determined accordingly. A quadratic modelcorrelating all the processvariablesconsidered with the

responsewas developed to fit the experimental results. The full quadratic model is given below in Equation 3:

$$Y = b_0 + b_1A + b_2B + b_3C + b_{12}AB + b_{13}AC + b_{23}BC + b_{11}A^2 + b_{22}B^2 + b_{33}C^2 \quad (3)$$

Where Y is the predicted output response (degradation efficiency); A is the initial MB concentration (mg/L); B is the catalystdose (g/L), and $C$is the Irradiation time(hours). Meanwhile, (b_0,b_1, b_2, and b_3), (b_{11}, b_{22},andb_{33}), and (b_{12}, b_{13}, and b_{23}) are the constant regression coefficientsfor the linear, interaction,and quadratic effects, respectively.

The analysis of variance (ANOVA) was used for the evaluation of the adequacy of the model developed and the statistical significance of the regression coefficients likewise Fisher's F-value was also used to examine the significance of theregression coefficients. Also, the coefficient of correlation (R^2) value was compared to the adjusted(R^2) value to check the adequacy of the model. A three-dimensional (3D) surface contour plot of the independent variables with the interactive effects on the corresponding responses was made using the Design expert (V12.0) to find the optimum values of the independent variables. Finally, the optimumvalues of the independent variables were determined using the same software.

Table 1:
Ranges of process parameters for the selected degradation factors

Variables (Unit)	**Factors**	**Levels**	
		-1	+1
Dye Conc. (mg/l)	A	5	35
Catalyst Dosage (g)	B	0.05	0.25
Time (hrs)	C	1	4

2.5. Artificial Neural Network Modelling

ANN has been of much interest in the modeling field and as a reliable computing method due to its ability to imitate the learning skills of biological cells or the human brain and its ability to learn more complex processes [18].

The Artificial NeuralNetwork (ANN) was also used to predict the output responses using MATLAB 2021b software to compare the responses generated by the CCD with the actual experimental values.TheNeural Fitting app (nftool) was used to select data, create, and train a network in the MATLAB software. The model parameters aredescribed as such; The feed-forward neural network witha back propagation method was used for the model development, and the training of the network was also done usingthe Levenberg-Marquardt Algorithm (LMA). The input layer will comprise three (03) neurons which are concentration (mg/L), dose (grams), time (hours), and different hidden layers of (1-30) neurons was tested for optima number of neurons while the output layer comprises one (01) neuroni.e. MB degradation Percentage (%).Finally, the mean square error (MSE)and the prediction performance wereevaluated using regression analysis coefficient (R^2), RMSE, and AARE [9, 21].

3. Results and discussions

3.1 Characterization of the Synthesized TiO_2-CuO/HAp catalyst
3.1.1X-Ray Diffraction (XRD) Analysis

The structural analysis of thehydroxylapatite (HAp), CuO, TiO_2 and the synthesized TiO_2-CuO/HAp composite determined by X-ray diffraction are presented in Fig. 3. From Fig. 3(a) Prominent peaks observed at $2\theta=26.5^0$,$32\text{-}35^0$ are attributed to the presence of the hydroxylapatite group [20] while Fig. 3(b) shows high peaks at $2\theta=35.2^0\text{-}38^0$indexing to CuO [42]. Similarly, Fig. 3(c) reveals the sharp peaks of Titanium. Finally, in Fig. 3(d) the XRD of the composite withdiffraction peaks at 2θ values of 25.3^0,37.8^0,47.6^0,55^0,$62.4^0$and 69.1^0 [19]can be indexed to anatase phase of TiO_2while other prominent diffraction peaks at $2\theta=35.5^0$,37^0,48.37^0 can be attributed to the CuOstructure and the discernible peaks at the $2\theta=26.3^0$,$32\text{-}35^0$ and $46.2^{0-}56^0$ are assigned to hexagonal phase of HAp [20]. This proves the presence of TiO_2, CuO, and HAp in the synthesized catalyst.

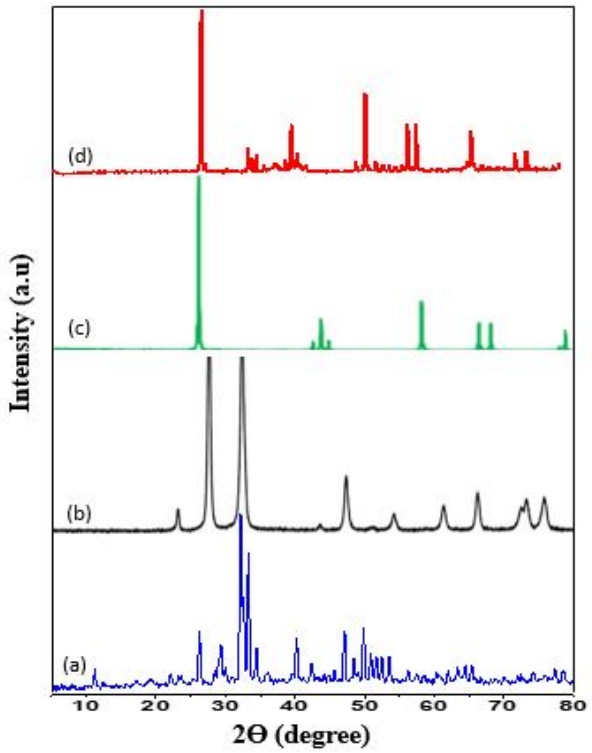

Fig. 3: The XRD patterns of (a) HAp (b) CuO (c) TiO_2 (d) TiO_2-CuO/HAp

3.1.2Scanning Electron Microscope (SEM) Analysis

Fig. 4 shows the morphology of the TiO_2-CuO/HAp asanalyzedvia scanning electron microscope (SEM). The SEM image shows a porous particle witha spherical shape, a relatively smooth flower-like surfacethat ishighly agglomerated into larger sizes[44].

Fig. 5 demonstrates the elemental composition as revealed by the EDS to be Cu, P, O, and Ti exist in TiO_2-CuO/HAp composite, and the Ca/P ratio as determined from the quantitative analysis of the atomic concentration was 1.67 [20].

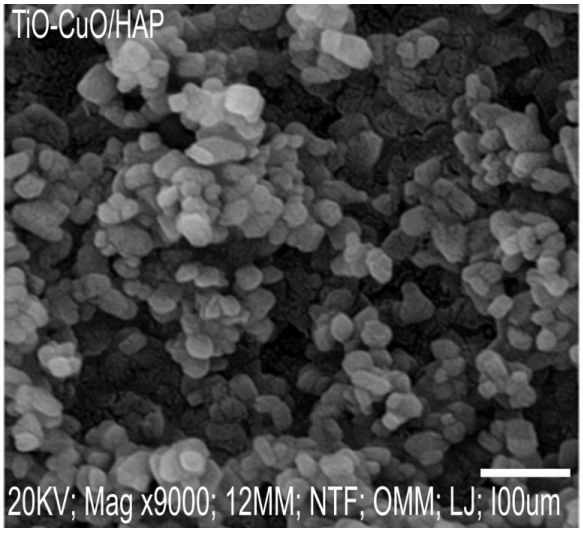

Fig. 4: SEM micrographs of TiO_2-CuO/HAp Catalyst

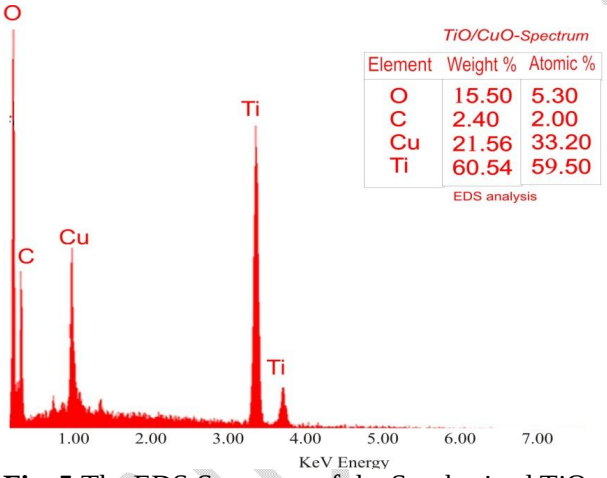

Fig. 5:The EDS Spectrum of the Synthesized TiO_2-CuO/HAp Catalyst.

3.1.3 Fourier Transform Infrared Spectroscopy (FTIR) Analysis

The Fourier Transform Infrared Spectroscopy (FTIR) Analysis was used to identify the surface functional groups present in TiO_2-CuO/HAp particles. Fig. 6 shows the FTIR spectra of the samples of HAp and TiO_2-CuO/HAp particles before and after the photodegradation experiment.

Fig. 6(a) reveals a sharp band at 1025 cm^{-1} which is associated with the phosphate group while the spread band of (C-O) at wave number 1350-1480 cm^{-1} is associated with the carbonate groups likewise the stretch band at 3250-3570 cm^{-1} signifies the presence of the hydroxyl group which confirms Hydroxyapatite (HAp).

Fig. 6(b) shows the presence of the phosphate group (PO_4^{3-}) at 1025-1090 cm^{-1} band and the O-H broad band observed at around 3200-3500 cm^{-1} proves the presence of hydroxide group in the composite. Similarly,after the photodegradation of MB (Fig. 6c), the intensities of the bands wereshifted from 1025

cm^{-1}, 1350.65 cm^{-1}, and 3375.20 $cm^{-1}$to 1024.10 cm^{-1}, 1350.32 cm^{-1}, and 3374.89 $cm^{-1}$for phosphate, carbonate,and hydroxyl group respectively.This shift in the peaks shows the binding of dye ions on the catalyst.

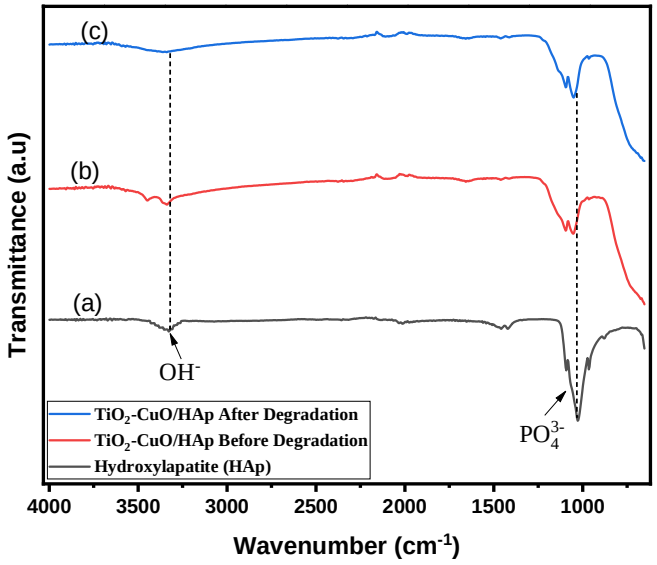

Fig. 6: (a) FTIR of pure HAp(b) FTIR of TiO_2-CuO/HAp sample before photodegradation experiment (c)FTIR of TiO_2-CuO/HAp sample after photodegradation experiment

3.2 RSM Modelling

3.2.1. Statistical analysis and model development

A study using RSM was performed to optimize the methylene blue degradation over the design level of 3 different variables and a total number of 20experimental runs.The photocatalytic experiments were performed according to Table 2. The generated data wereanalyzed using three levels of CCD of the Design Expert version 12.0 software and then interpreted while repeated runs were also used to confirm the experimental errors.The response is the percentage of methylene blue degradation.For a specific experimental run, the actualresponse values obtained were close to the predicted values (Table 2).The experimental investigations were described by a quadratic model with a design expert thatprovided the below regression as shown in Eq. 4 in both actualfactors for methylene blue degradation (%).

MB Degradation Percentage(Y) = 75.0505 + 0.914199*A + 22.70501*B + 12.07893*C + 1.113333* A*B - 0.08944*A*C - 3.26667* B*C - 0.02543*A^2 - 165.82* B^2- 1.77745* C^2(4)

Where A= Dye concentration, B= Catalyst Dosage, and C= Irradiation Time.

Eq. 4 predicted the experimental results of MB degradation (%)as described also in Table 2. The accuracy and significance of the suggestedmodel were analyzed by ANOVA. The results show an excellent agreement between the experimental and predicted values.

Table 2. *Experimental design matrix for MB degradation on TiO_2-CuO/HAp catalyst and response*

Runs	A:Dye Concentration (mg/l)	B:Catalyst Dosage (g)	C:Irradiation Time (hour)	Response Degradation (%)		
				Experimental	RSM Predicted	ANN Predicted
1	35	0.05	1	86.42	85.57	86.25
2	35	0.05	4	86.16	85.26	86.12
3	20	0.318179	2.5	92.29	92.13	91.89
4	5	0.25	1	85.55	84.72	85.47
5	45.22689	0.15	2.5	79.53	79.35	79.56
6	5	0.05	4	97.91	97.42	97.18
7	20	0.15	2.5	99.89	99.57	99.23
8	20	0.018179	2.5	98.76	98.38	98.85
9	5	0.25	4	89.58	90.51	90.36
10	5	0.05	1	89.03	89.67	89.38
11	20	0.15	5.022689	91.04	90.56	91.13
12	35	0.25	1	86.73	87.30	86.96
13	5.22689	0.15	2.5	96.5	96.37	96.76
14	20	0.15	2.5	99.92	99.56	99.87
15	20	0.15	0.022689	86.02	86.40	86.56
16	20	0.15	2.5	98.97	99.57	99.89
17	20	0.15	2.5	99.98	99.58	99.86
18	20	0.15	2.5	99.98	99.56	99.82
19	20	0.15	2.5	98.5	99.57	99.89
20	35	0.25	4	85.60	85.04	85.57

3.2.2 Model fitting and ANOVA analysis

Table 3shows the ANOVA results for the developed response surface quadratic model. It indicates the relationship and statistical suitability of the quadratic model developedfrom the RSMwhich is for the representation of the process of MB photodegradation on TiO_2-CuO/HAp catalyst during the study.The

suggested response model's efficiency degreewas determined by P-value, R^2, F-value, and adjusted R^2. The model Fisher's F-value of 129.01implies that the model is significant. Moreover, the P-values less than 0.050 indicate thatthe model terms are significant. Hence, A, B, C, AB, AC, A^2, B^2,and C^2 are the significantmodel terms while lack of fit withan F-value of 2.52 implies that the Lack of Fit is not significant. The F value of 83.52 shows that MB concentration has the most influence as an individual parameter on MB degradation. Furthermore, the proposed model fits the experimental results which can be confirmed by the correlation coefficient (R^2) value which is near 1. In this study, the R^2 value (0.9915) which is close enough to the adjusted R^2 value (R^2_{adj}=0.9838) has a reasonable agreement. Lastly,the experimental work reliability and accuracy could be explainedby a coefficient of variance (CV) of 0.9225% (< 10%) [22].Fig. 7 (a) reveals a good agreement ofactual values with predicted values for MB degradation, the actual values were relatively distributed closely to the straight line which could be a show of the adequacy of the regression model.Furthermore, Fig.7(b)shows the normal probability plotting of the studentized residuals. It can bededuced from the graph that many data points were closely associated along the straight-line region with no much deviation from the line. Hence, thenormality assumption was satisfied from the residual plotwith no individual residuals passing the residual variance[17,23].Moreover, Fig. 7 (c) and Fig. 7 (d) showsthe residuals vs. run were a useful diagram for understanding variables that may influence the response during experimentation while the plotof residuals vs. predicted values was used to test for the acceptance of constant variance.

Table 3: ANOVA result for the response surface quadratic model

Source	**Sum of Squares**	**Df**	**Mean Square**	**F-Value**	**P-Value**	
Model	842.35	9	93.59	129.01	< 0.0001	Significant
A-Dye Concentration	60.59	1	60.59	83.52	< 0.0001	
B-Catalyst Dosage	20.25	1	20.25	27.92	0.0004	
C-Irradiation Time	25.41	1	25.41	35.02	0.0001	
AB	22.31	1	22.31	30.75	0.0002	
AC	32.40	1	32.40	44.66	< 0.0001	
BC	1.92	1	1.92	2.65	0.1348	
A^2	292.91	1	292.91	403.74	< 0.0001	
B^2	29.23	1	29.23	40.28	< 0.0001	
C^2	227.08	1	227.08	313.01	< 0.0001	
Residual	7.25	10	0.7255			
Lack of Fit	5.19	5	1.04	2.52	0.1666	not significant
Pure Error	2.06	5	0.4121			
Cor Total	849.60	19				

R^2= 0.9915
Predicted R^2 =
0.9225Adjusted R^2 = 0.9838
Adequate precision

=33.5585
C.V. (%) = 0.9225

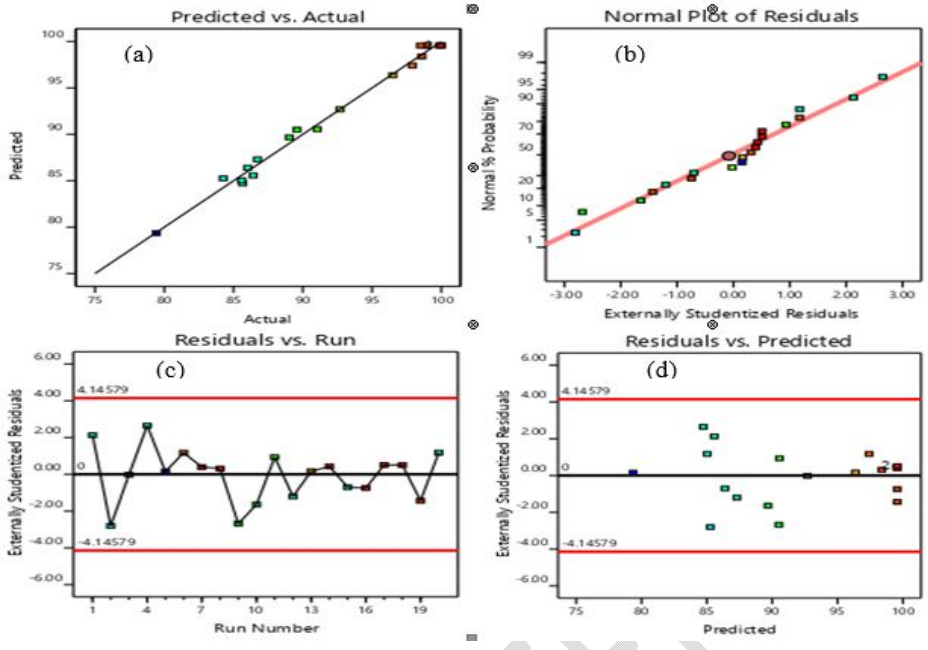

Fig. 7: (a) predicated vs actual, (b) Normal plot of residual, (c) residual vs run, and (d) residual vs predicated for percentage methylene blue degradation.

3.2.3Response surface plots

Three-D response surface plots can be explained as a graphical depiction of theregression model equation used to explain the optimum conditions offactors and are mostly applied to establish the type of interactions between variables used and for enhanced understanding for maximum efficiency.
Fig.8(a–b) represents the effect of the three independent factorswhich are the concentration MB, Irradiation time, dose and the responseapplied. In each 3D response surface plot, onefactor was fixed at the corresponding zero level whilethe remaining two factors were changed within the experimental ranges.Fig 8 (a) represents the influence of catalyst dosage and concentration on methylene blue degradation. From the result, an increase in catalyst dosagefrom (0.05 to 0.15) and concentration increases the efficiency smoothly to (97.5%) and then decreases with increasing the dosage and concentrationfrom (0.15 to 0.25) which may be attributed to the surface of the active sites getting saturated more with the catalyst particles thereby decreasing the reaction rate and mass transfer [9].Similarly,Fig. 8(b) represents the influence of time and dosage on MB degradation. The irradiation time has a significant effect on the degradation rate, as shown in the plot, an increase in the irradiation time up to 2.5 hoursincreases the degradation efficiency while a further increase in the time to 4 hoursleads to a decrease in the efficiency.The increase in MB degradationefficiency with TiO_2-CuO/HApcatalyst dose and dosage initially is due to the availability of more active sites for the trapping of the dye and the presence of enough time for the adsorption in darkness and photodegradation process thereafter in the light [45].

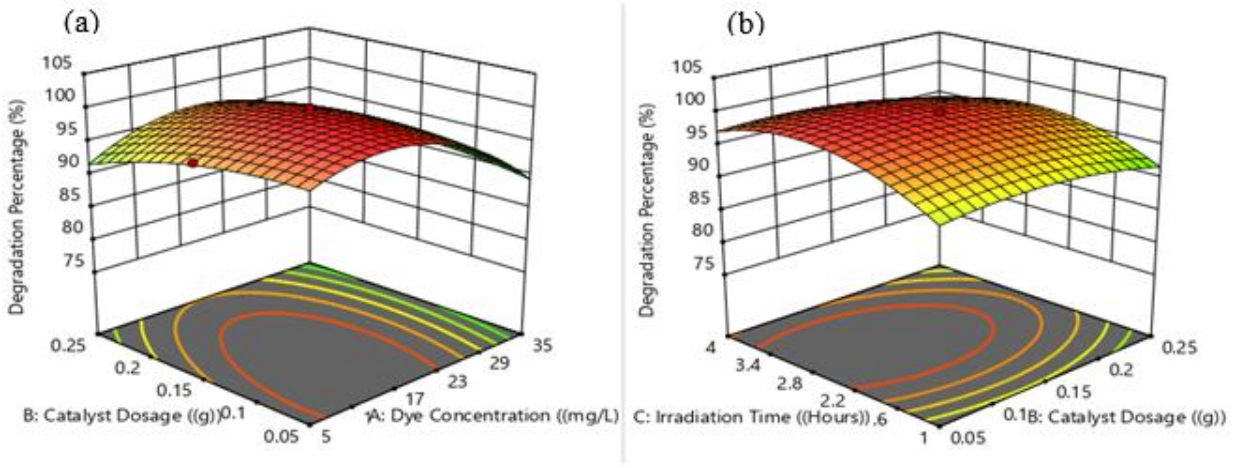

Fig. 8: The response surface plot of methylene blue degradation as the function of (a) Dosage and concentration (mg/L) (b) Time (Hours) and dose (g/L)

3.3 ANN Modelling

The Artificial Neural Network (ANN) was successfully applied to predict the system's behavior and thedegradation (%) of methylene blue.The multilayer perceptron (MLP) network was developed in MATLAB (The Works Inc. 2018b) using theback propagation algorithm to train the feed-forward neural network. The Levenberge–Marquardt Algorithm (LMA) was also used because it has the least MSE. The Neural Fitting app (nftool) was used to select data, train the network, data validation, and test.
The input data for training were obtained from theexperiments via the CCD with three input neurons which are theindependent variables (initial MBconcentration (mg/L), Irradiation time (hours), TiO_2-CuO/HAp dose (grams), Different number of neurons in the range of 1-30 was tested in the hidden layer, the network with 20 neurons in hidden layer had the best results of minimal error (RMSE=0.56) and higher R^2 value (R=0.9984) for the training and (R=0.9939) for testing data. Therefore, in this study, a three-layeredfeed-forward-back propagation neural network (3:20:1) was used for the modeling of the degradation process and the network was trained after some iterations. The data set from the total runs was divided into 70% which was used fortraining the network while the remainingdata was divided into 15% for the validation and 15% for the testingof the network. The regression analysis coefficient (R^2), root mean square error (RMSE), and absolute average relative error (AARE) were also usedin evaluating itsprediction performance.

The mathematical expression of all these parameters is defined inEqs. (5–7). Furthermore, Table 2 shows the predicted responses from the ANN modeling technique. Finally, Fig. 9 shows the linear fit model obtained by the plot of the ANN training, testing, and validation outputs, Y versus the targets T, the values of R^2 for each of the outputs are shown on the plots. An overall regression coefficient of R^2=0.9976 was obtained which is close to unity indicating a better relationship of the data.
The linear fit model obtained from the plot of the ANN validation and Targets, T which was used to predict the ANN model output responses was also given by the respective output equations on the plots (Fig.9).

$$R^2 = 1 - \frac{\sum_{i=1}^{N}(\mathrm{PRi} - OBi)^2}{\sum_{i=1}^{N}\mathrm{PRi} - OBi)^2} \quad (5)$$

$$\mathrm{RMSE} = \sqrt{\sum_{i=1}^{N}\frac{(PRi - OBi)^2}{n}} \quad (6)$$

$$\mathrm{AARE} = \frac{\sum_{i=1}^{N}(\frac{Pi - Oi}{Oi})}{n}\ x\ 100 \quad (7)$$

Where *PRi*is the predicted values for either ANN or RSM, *OBi*isthe experimental/observed values, *n* is thenumber of samples, *Pm* is the average values, *Pi* is the predicted values obtained either from ANN or RSM and *Oi* isthe experimental/observed values.

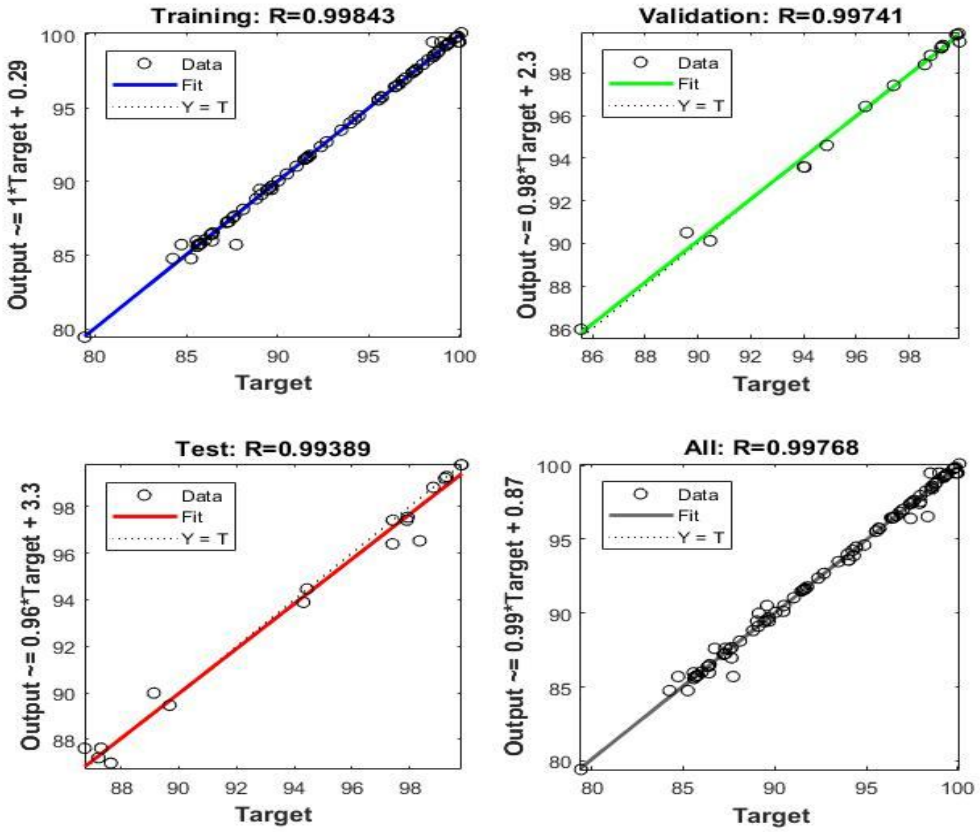

Fig. 9. The MATLAB interphase for ANN training, testing, and validation

3.4 Evaluation of RSM and ANN models and Validation

The comparison of ANN and RSM for the modeling of methylene blue degradation was made based on some parameters such as R^2, RMSE, and AARE. The ANN model has a higher value of R^2 and close to 1 than the RSM while the RMSE and AARE values are also lower. The results of the comparison of these parameters (R^2, RMSE, and AARE) for ANN and RSM models as calculated by equations (5-7) can be seen in Table 4.

Table 4: Performance parameters as obtained for ANN and RSM models

Parameters	ANN	RSM
R^2	0.9973	0.9915
RMSE	0.4980	0.6100
AARE	0.0013	0.0245

For a well-fitted model, the values of R^2 must be close to 1, thevalues of RMSE must be close to zero while values of AARE must also be small as possible. It should be noted that larger values of these AARE and RMSE mean larger chances of errors in the respective predictions.
The predicted ANN model was well-fitted to the experimental data more than the RSM model-based prediction becausethe ANNmodel was able to capture the nonlinearities of theexperimental data better than the RSM model. Hence, the prediction efficiency and performance of ANN viathe neural network has a better accuracy for the modeling of photocatalytic degradation of methylene blue as compared to RSM which can be associated with its universal capability.
For model validation, the optimal conditions of the three process variables which aremethylene blue concentration, time,and dosefor degradation wereinvestigated basedon the desirability function through the RSM technique. According to the optimization result, the optimalconditions for maximum methylene blue degradation efficiency (99.62%) wereestablished to be, the irradiation time of 2.5hours (150 mins), TiO_2-CuO/HAp dose of 0.15 g, and initial methylene blue concentration of 20 mg/L with the desirability of 1.00 aspresented in Table 5. The good agreement between the predicted andexperimental results confirms model validation tosimulate the methylene blue degradation.

Table 5: The Optimum value of process parameters and their experimental conditions

		Methylene blue degradation (%)		
Variables	**Optimum Values**	**Predictive**	**Experimental**	**Desirability**
Time	2.5hrs	99.50	99.62	1.00
Dose	0.15g			
Concentration	20mg/L			

3.5 Reaction kinetics study

The reaction kinetics of photocatalytic degradation showsthe rate of pollutants uptake onto the photocatalyst. It describes the adsorption kinetics of solutes on a solid surface and as well controls theequilibrium time for reaction [24].The various kinetic models engaged in this study which are thepseudo-first-order, and pseudo-second-order models [25] as well as the intraparticle diffusion kinetic model for the diffusion mechanism [26] are presented below.

3.5.1 Pseudo-first order kinetic model

The Lagergren equation is the earliest known model describing the adsorption rate in solute-adsorbent systems and is widely used for the pseudo-first-order(PFO) kinetics.Fig. 10(a) describes the Lagergren

PFO model of the photocatalytic degradation kinetics of methylene blue usingTiO_2-CuO/HAp. The Lagergren (Pseudo-first order)equation is defined in Eq. (8)

$$\log(q_e - q_t) = logq_e - \frac{K_1 t}{2.303} \quad (8)$$

Where q_e and q_t (milligrams per gram) are the amounts of MB adsorbed or adsorption capacity at equilibrium and at any time t (min) respectively.The k_1 values which is the rate constant of pseudo-first-order adsorption are obtained from the slopes of linear plots of log (q_e-q_t) versus the time t[27,28].
The plots were found linear with good correlation coefficients (R^2= 0.9145) for the pseudo-first-order kinetic model and the results from the linear curve of the plot were analyzedand other parameters are presented in Table 6.

3.5.2. Pseudo-Second order kinetic model

The pseudo-second-order (PSO) kinetic model was also used to describe the adsorption kinetics of MBon TiO_2-CuO/HAp catalyst as shown in Fig. 10(b). The pseudo-second-order kinetic equation is expressed as;

$$\frac{t}{q_t} = \frac{1}{K_2 q_e^2} + \frac{t}{q_e} \quad (9)$$

WhereK_2 is the pseudo-second-order adsorption rate coefficient (g/mg min), q_e and $q_t$remain the adsorption capacity at equilibrium (mg/g) and at time t (mins) respectively. Fig. 10(b) shows a linear plot of q_t vs t which gave a correlation coefficient R^2 with other values of constants (Table 6) as obtained from the slope and intercept of the plot [27-29].Finally, from the results of the reaction kinetic plots, the pseudo-second-order fitted the experimental data well, moreover,the correlation coefficient, R^2 values for the pseudo-second-order model (Table 6 and Fig. 10b)shows excellent linearity and close to unity(R^2= 0.9950)than that of the pseudo-first-order model (R^2= 0.9145). This suggests to us that the degradation of MB using TiO_2-CuO/HApfollowed the pseudo-second-order rate expression well andis chemisorption in nature [35,17].

3.5.3. Intraparticle diffusion kinetic

The intraparticle diffusion model as proposed by Weber and Morris was also used in the analysis of the adsorption kinetic i.e. the diffusion mechanism of the adsorbate through the solution[30]. Investigation of rate controlling step is considered as an important factor in a photocatalytic degradation process.Hence, the photo-degradationprocess of pollutant molecules over the surface of the photocatalyst is known to involve three steps: (1) mass transfer of pollutant/dye across theexternal boundary layer (film or external diffusion) (2) the intraparticle diffusion along the photocatalyst pores (pore diffusion) and(3) photocatalytic degradation at the sites on the surface of the photocatalyst (surface diffusion). Usually,either the intraparticle diffusion or film, surface,or the association of more than one of thesemechanisms controls the overallphotocatalytic degradation rate [30-32]. The intraparticle diffusion rate was described using equation 10;

$$q_t = K_{id} t^{1/2} + C \quad (10)$$

Where qt is the amount in (mg/g) of MB adsorbed at sorption time t (min), K_{id} is the intraparticle diffusion rate constant (mg/gmin$^{1/2}$) and the constant C which is related to the thickness of the boundary layer can be obtained from the slope and intercept of the plot qt versus $t^{1/2}$. The kinetic data were processedto determine whether the intraparticle diffusion was the rate-limiting step. If the Weber–Morris [33] plot of *qt* versus $t^{1/2}$ gives a straight line, thenthe sorption process is controlled by intra-particle diffusiononly. However, if it exhibits multi-linear plots, thentwo or more steps control or influence the sorption process. From the results obtained the values of constant *C, the* correlation coefficient $R^{2,}$and intraparticle diffusion rate constant K_{id} are presented in Table 6. Fig. 10(C) shows the linearized form of the intraparticle diffusion model, the linear curve of the plot shows the diffusion of the dye through the solution to the surface of the catalyst where intraparticle diffusion of the dye on the surface of the catalyst takes place alone and hence, the external or film diffusion is assumed negligible in the process [34].

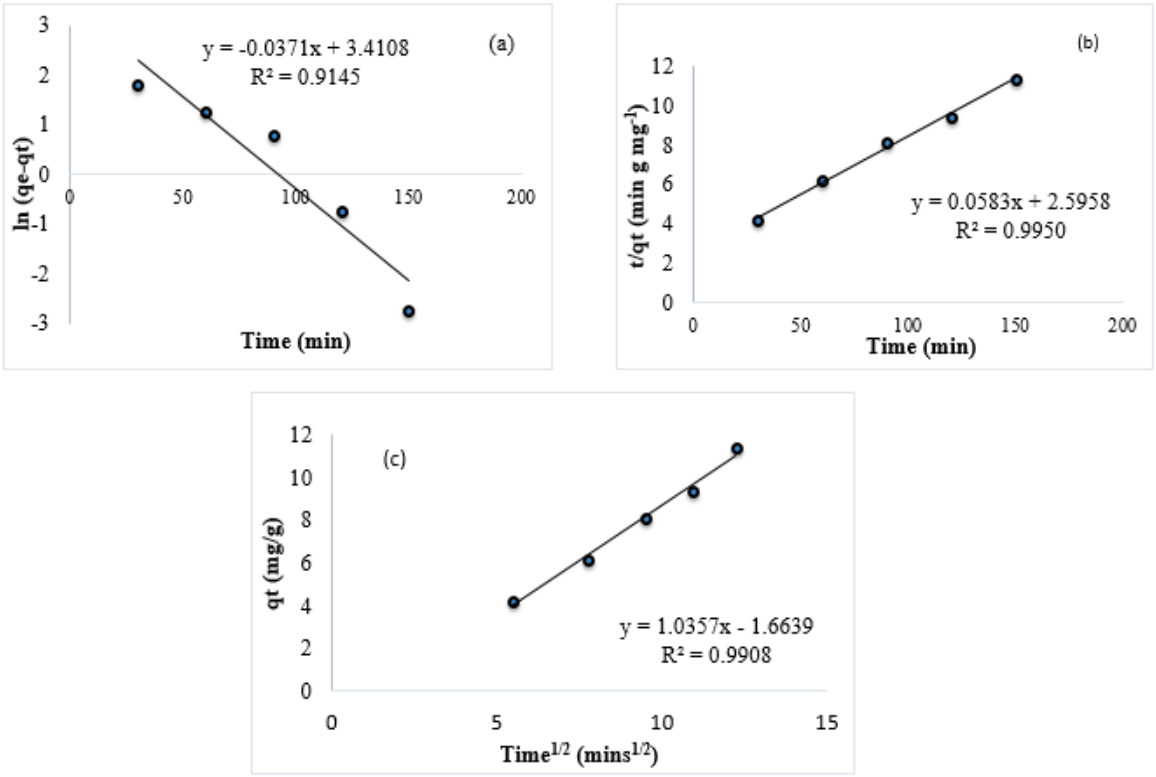

Fig. 10 (a) *Pseudo-first-order (b) Pseudo-second-order and (c) Intraparticle diffusionkinectic models for photocatalytic degradation of methylene blue using TiO_2-CuO/HApcatalyst*

Table 6:
Kinetic study of methylene blue degradation using TiO_2-CuO/HAp Catalyst

Model	Model Equation	Plots	Kinetic Parameters
Lagergren Firstorder	$\ln(qe-qt) = \ln qe - K_1 t$	$\ln(qe-qt)$ Vs t	k_1 (min^{-1}) = 0.0371 q_e (mg/g) =30.289 R^2=0.9145
Pseudo Second order	$t/qt = 1/k_2 qe^2 + t/qe$	t/qt Vs t	k_2 ($gmg^{-1}min^{-1}$) = 0.0013 q_e (mg/g) =17.15 R^2=0.9950
Intraparticle Diffusion	$q_t = K_{id}\, t^{1/2}$	$t^{1/2}$ Vs q_t	K_{id}($mgg^{-1}min^{-1(1/2)}$) = 1.035 C(mg/g) =1.663 R^2=0.9908

3.6 Adsorption Isotherms Study

The adsorption isotherm plays a significant role in any adsorption process by providing information on the adsorbent and adsorbate affinity and understanding the degradation or removal mechanisms depending on the purpose, especially for a large-scale application. The isotherms help to design suitable experimental systems and to also find out any deviation between experimental data and the isotherm models.
In this work, the equilibrium data from the adsorption isotherm experiments were analyzed with Langmuir, Freundlich, Temkin, and Redlich-Peterson models.

3.6.1 Langmuir Adsorption Isotherm

The Langmuir adsorption isotherm was used to analyze the experimental data according to the non-linear equation represented eq. 11.

$$q_e = \frac{q_m K L C_e}{1+KLC_e} \qquad (11)$$

Where Ce= dye concentration at equilibrium (mgL^{-1}); qe = equilibrium adsorption capacity ($mg\ g^{-1}$); K_L = Langmuir adsorption constant ($L\ mg^{-1}$); q_m = maximum adsorption capacity (mgg^{-1}). Furthermore, a dimensionless separation factor called equilibrium parameter R_L is also an essential characteristic of the Langmuir isotherm which can be expressed as;

$$R_L = \frac{1}{1+K_L Ce} \quad (12)$$

Where K_L remains the Langmuir adsorption constant (Lmg^{-1}) and Ce is the dye concentration at equilibrium (mgL^{-1}); the parameter R_L signifies the shape or type of isotherm as follows with value of R_L>1 Unfavorable, R_L=1 Linear, 0<R_L<1 Favorable, R_L=0 Irreversible respectively.
Fig. 11(a) shows the plot of Ce/qe vs Ce which fitted well with the experimental data to give a linear plot with a correlation coefficient of R^2=0.9964. The slope and intercept of the plot were used to calculate other Langmuir isotherm parameters which include q_m=0.9524mg/g, K_L=6.195L/mg, and R_L=0.01065 (Table 7).

3.6.2 Freundlich Adsorption Isotherm

The Freundlich adsorption isotherm model was also used to analyze the experimental data. The model equation is given as equation 13;

$$q_e = K_f C_e^{\frac{1}{n}} \qquad (13)$$

Where qe = equilibrium adsorption capacity (mgg^{-1}), Ce = dye concentration at equilibrium (mgL^{-1}); K_f= Freundlich constant (mg/g)*(L/mg)^$^{1/n}$; n= heterogeneity factor of adsorption sites (dimensionless); A straight line graph from the plot of ln (qe) vs ln (Ce) will give a slope equal 1/n and intercept ln (K_f). The reciprocal 1/n can have values between 0 and 1, thus when n>1, it is favorable adsorption[43],andwhen 1<n<10, it is a beneficial adsorption condition[46,47].

Fig.11 (b) shows a linear plot of ln (qe) vs ln(Ce)witha correlation coefficient of R^2= 0.9873. The Freundlich parameters were also calculated from the slope and intercept of the curve; thus, K_F=1.4063mg/g and n=2.50 as shown in Table 7.

The plot results from the above two models show that the Langmuir isotherm with a higher correlation coefficient close to unity fits well with the experimental data than the Freundlich isotherm model. Hence, the highercorrelation coefficient value of 0.9964 suggests that the Langmuir isotherm mightbe a more suitable isotherm model. It was thus concluded that the adsorptionprocess of methylene blue onto the TiO_2-CuO/HAp catalyst exhibited a monolayer adsorption process.

3.6.3 Temkin Adsorption Isotherm

The Temkin isotherm model as represented by Eq. 14was used to fit the experimental data likewise.

$$q_e = \frac{RT}{b} \ln(A_T C_e) \qquad (14)$$

Where A_T (Lg^{-1}) is the Temkin isotherm constant, b (J mol^{-1}) is a constant related to the heat of sorption and R= (8.314 J mol^{-1} K^{-1}) is the gas constant, T= Temperature (Kelvin). Thus, Fig.11(c) shows the plot of qe vs Ln Ce with a correlation coefficient of R^2= 0.9719 from which other Temkin parameters were calculated from the slope and intercept of the curve.

3.6.4 Redlich - Peterson Adsorption Isotherm

Redlich-Peterson Isotherm model is an empirical isotherm incorporating three parameters. It combines elements from both Langmuir and Freundlich equations; therefore, it is a mix-mechanism of adsorption and does not necessarily follow the ideal monolayer adsorption [37]. The model is described by Eq. 15.

$$q_e = \frac{K_{RP}C_e}{(1+\alpha_{RP}Ce^{\beta})} \qquad (15)$$

Where Ce is equilibrium liquid-phase concentration of the adsorbent (mgl^{-1}) and qe is equilibrium adsorption ($mg\ g^{-1}$), $K_{RP}$is Redlich-Peterson isotherm constant (Lg^{-1}),α_{RP} is constant (Lmg^{-1}), β is Redlich - Peterson exponent that lies between 0 and 1. It should be noted that at high liquid-phase concentrations of the adsorbate, Eq. 15 reduces to the Freundlich equation [38] and when β=1, it reduces to Langmuir equation [39].

$$q_e = \frac{K_R Ce^{1-\beta}}{\alpha_R} \qquad (16)$$

Fig. 11(d) described the linear plot of lnC_e/qe Vs lnC_e for Redlich – Peterson model, whereby in the determination of Redlich-Peterson constants, β is slope and K_{RP} is intercept [40,41]. The correlation coefficient is (R^2=0.9901) and while other parameters from the plot were evaluated and presented in Table 7.

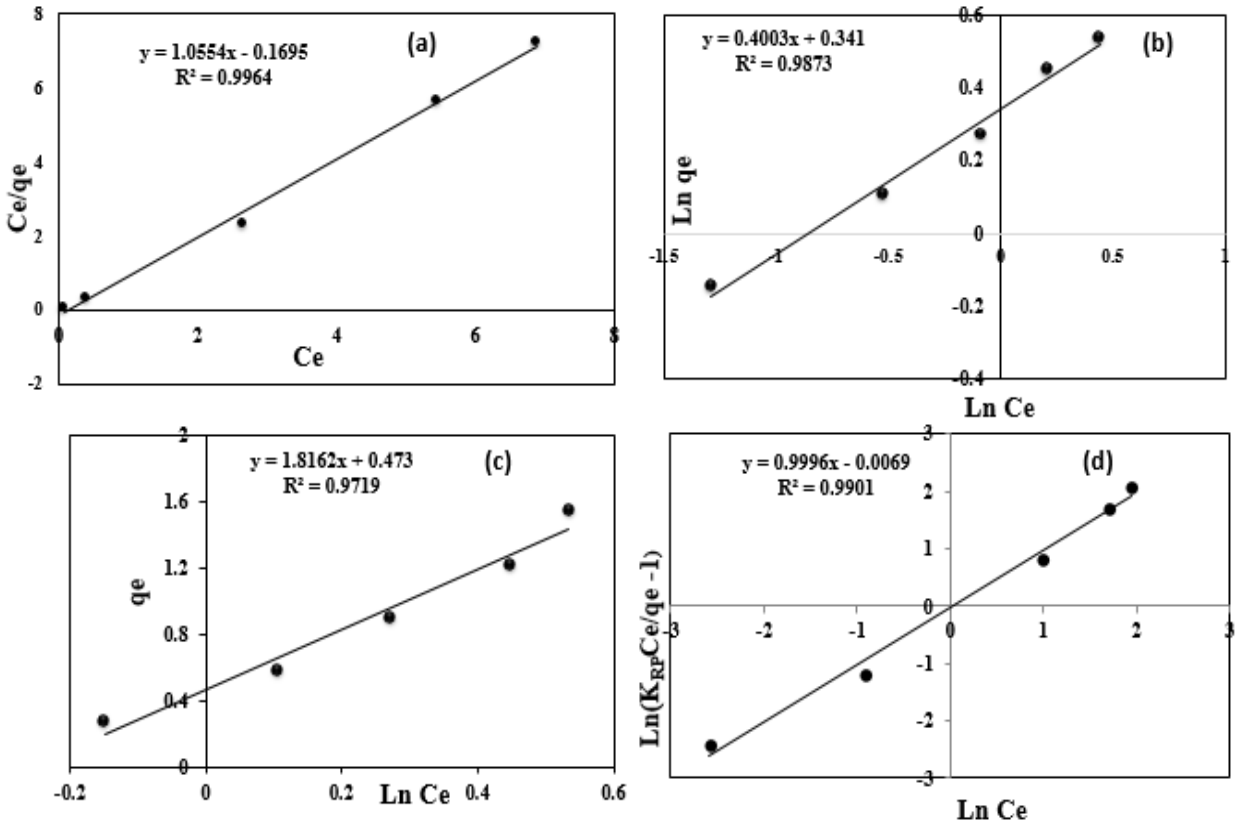

Fig. 11 (a)TheLangmuir, (b) Freundlich, (c) Temkin and (d) Redlich Peterson isotherm models for photocatalytic degradation of methylene blue using TiO_2-CuO/HAp Catalyst

Table7
Adsorption Isotherms for Methylene Blue Degradation on TiO_2-CuO/HAp Catalyst at temperature 298K

Isotherms	**Model**	**Linear Form**	**Plots**	**Kinetic Parameters**
Langmuir	$q_e = \frac{q_m K L C_e}{1 + K L C_e}$	$\frac{C_e}{q_e} = \frac{1}{q_m K_L} + \frac{C_e}{q_m}$	Ce/qe vs Ce	q_m=0.9524mg/g K_L=6.195L/mg, R_L=0.01065 R^2=0.9964
Freundlich	$q_e = K_f C_e^{\frac{1}{n}}$	$Lnq_e = LnK_F + \frac{1}{n} LnC_e$	ln qe vs ln Ce	K_F=1.406mg/g n=2.500 R^2= 0.9873
Temkin	$q_e = \frac{RT}{b_T} \ln(A_T C_e)$	$q_e = \frac{RT}{b_T} LnA_T + \frac{RT}{bT} LnC_e$	qe vs ln Ce	A_T=2.344 L/g b_T=6.189 kJ/mol R^2= 0.9719
Redlich – Peterson	$q_e = \frac{K_{RP} C_e}{(1 + \alpha_{RP} Ce^{\beta})}$	$\frac{C_e}{q_e} = \frac{1}{K_{RP}} + \frac{\alpha_{RP}}{K_{RP}} C_e^{\beta}$	$\ln(K_{RP} \frac{Ce}{q_e} - 1)$ Vs $\ln C_e$	β= 0.9890 K_{RP}= 1.0069 L/g α_{RP}=0.0069 Lmg^{-1} R^2=0.9901

4.0 Conclusions

The photodegradation of methylene Blue (MB) using TiO_2-CuO/HApcatalyst was studied. The TiO_2-CuO/HAp was successfully synthesized and characterized with FTIR, XRD, SEM and EDX.The effects of different process variables such as Irradiationtime, catalyst dose and initial MB concentration maintained at pH=8for the degradation of MB using TiO_2-CuO/HAp catalyst were investigated using the central composite design (CCD) method. Thecapabilities of the Response Surface Methodology (RSM) and Artificial Neural Network (ANN)modeling methods in predicting the output response (MB degradation efficiency) were examined and the ANN was found capable of having ahigher prediction ability for MB degradation at various operating parameters as compared to the RSM model.Theeffects of the process variables and their optimum conditions were determined. Theadsorption data were fitted into different isotherms and kinetics models. The ANN model was found to bemore acceptable since it has a higher R^2 value and lower RMSE and AARE compared to the RSM values even though both can beapplied for the prediction of the output (MB degradation efficiency). Optimum MB degradation efficiency of 99.62% was obtained at contact time of 2.5hours (150 min), TiO_2-CuO/HAp dose of 0.15g, and MBconcentration of 20mg/L. The experimental data fitted well with the pseudo-second-order kinetic model and Langmuir isotherm than the other models and Isotherms respectively.Hence, from this present study, it can be concluded that the prepared TiO_2-CuO/HAp can be used for the degradation of MB and the process can alsobe optimized.

5.0Abbreviations

ANN	Artificial neural network	PSO	Pseudo Second Order
AOPs	Advance Oxidation Process	pH_{PZC}	pH at point of zero charge
AARE	Absolute Average Relative Error	Qe	Amount of phenol adsorbed per unit mass of adsorbent (mg/g)
A_T	Temkin isotherm constant (L/g)	Qt	Amount of methylene blue adsorbed at any sorption time (t) (mg/g)
b	Temkin constant related to the heat of sorption (J mol^{-1})	q_m	Langmuir maximum degradation capacity (mg/g)
C	Constant associated with Boundary layer thickness	R	Universal gas constant (J/mol K)
CCD	Central composite design	R^2	Correlation coefficient
Ce	Equilibrium concentration of methylene blue (mg/L)	RMSE	Root Mean Square Error
C_t	Instantaneous methylene blue concentration, (mg/L)	R_L	Separation factor called equilibrium parameter
Co	Initial concentration of methylene blue Concentration	RSM	Response surface methodology
C_f	Final concentration of methylene blue Concentration	T	Absolute solution temperature (K)
DES	Design of Experiment Software	K_{RP}	Redlich-Peterson isotherm constant (Lg^{-1})
K_1	Adsorption rate constant of Psuedo first order kinetic model (g/mg min)	α_{RP}	Constant relating to Redlich-Peterson isotherm equation (Lmg^{-1})
K_2	Adsorption rate constant of the Psuedo second order kinetic models (L/min)	β	Redlich - Peterson exponential
K_{id}	Intraparticle diffusion rate constant ($mg/gmin^{1/2}$)	PFO	Pseudo First Order
K_D	The distribution coefficient	K_F	Freundlich isotherm constant related to degradation
K_L	Langmuir constant related to energy required for degradation (L/mg)	N	Freundlich exponential coefficient factor representing heterogeneity factor of adsorption sites

Declarations

Availability of data

The research data associated with this paper cannot be shared at this time due to privacy reasons and ongoing research.

References

[1]Khan, M. D., Singh, A., Khan, M. Z., Tabraiz, S., Sheikh, J.(2023).Current perspectives, recent advancements, and efficiencies of various dye-containing wastewater treatment technologies, *Water Process Engineering*,53, 103579. https://doi.org/10.1016/j.jwpe.2023.103579

[2] Cheng, J., Zhan, C.,Wu, J.(2020) Highly efficient removal of methylene blue dye from an aqueous solution using cellulose nano-fibrous membranes modified by polydopamine, *ACS Omega* ,5 (10), 5389–5400.https://doi.org/10.1021/acsomega.9b04425

[3]Katheresan, V., Kansedo, J.,& Lau, S. Y. (2018). Efficiency of various recent wastewater dye removal methods: A review. *Journal of EnvironmentalChemical Engineering*,6,4676-4697 https://doi.org/10.1016/j.jece.2018.06.060

[4] Habtamu, A.&Ujihara, M. (2023). The mechanism of water pollutant photodegradation by mixed and core-shell WO_3/TiO_3 nanocomposites, *RSC Adv.*,13, 12926-12940. https://doi.org/10.1039/D3RA01582C

[5] Rodríguez-Couto, S., Osma, J. F., Toca-Herrera, J. L. (2009). Removal of synthetic dyes by an eco-friendly strategy, *Eng. Life Sci.*, 9(2), 116–123, https://doi.org/10.1002/elsc.200800088

[6] Dawood, S., Sen, T.K. (2014). Review on dye Removal from its aqueous solution into alternative cost-effective& non-conventional adsorbent. *J. Chem. Proc. Eng.*, 1, 1-11, https://doi.org/10.17303/jce.2014.105

[7] Holkar, C.R., Jadhav, A.J., Pinjari, V.D., Mahamuni, N.M, Pandit, A.B. (2016). A critical review on textile wastewater treatments: Possible approaches. *Journal of Environ. Manag.*, 182, 351-366, https://doi.org/10.1016/j.jenvman.2016.07.090

[8]D'Antoni B.M. Iracà, F., Romero, M.(2017). Current treatment technologies and practical approaches on textile wastewater Dyes Removal, *Panterei water solutions*, 1-10, https://doi.org/10.13140/RG.2.2.11472.71689

[9]Zulfiqar, M., Samsudin, M.F.R., Sufian, S. (2019). Modelling and optimization of photocatalytic degradation of phenol via TiO_2 nanoparticles: An insight into response surface methodology and artificial neural network:A Chemistry, Journal of Photochemistry and Photobiology,384, 1-15, https://doi.org/ 10.1016/j.jphotochem.2019.112039

[10]Xu, S., Ng, J., Zhang, X., Bai, H., Sun, D.D. (2011). Adsorptionand photo-catalytic degradationof Acid Orange 7 over hydrothermally synthesized mesoporous TiO_2 nanotube,Colloids Surf. A Physicochem.Eng. Asp., 379,169–175.https://doi.org/10.1016/j.colsurfa.2010.11.032

[11] Singh,P.,Borthakur,A. (2018). A review on biodegradation & photocatalytic degradationof organic pollutants: a bibliometric and comparative analysis, *J. Clean. Prod.*, 196, 1669–1680.https://doi.org/10.1016/j.jclepro.2018.05.289

[12]Zhang, J., Fu, J., Dai, K. (2022). Graphitic carbonnitride/antimonenevan der Waals heterostructure with enhanced photo-catalytic CO_2reduction activity. *J. Mater. Sci. Technol.*, 116, 192–198. https://doi.org/10.1016/J.JMST.2021.10.045

[13] Chan, S.,Wu, TY., Juan, J.C., Teh, C.Y. (2011). Recentdevelopments of metal oxide semiconductors as photocatalysts in advanced oxidation processes(AOPs) for the treatment of dye wastewater. *J. Chem. Technol. Biotechnol.*, 86, 1130-1158.https://doi.org/10.1002/jctb.2636

[14] Vasiljevic, Z.Z., Dojcinovic, M.P., Vujancevic, J.D., Jankovic-Castvan, I., Ognjanovic, M.,Tadic, N.B., Stojadinovic, S., Brankovic, G.O., Nikolic, M.V. (2020). Photocatalytic degradation of methylene blue under natural sunlight using Irontitanate nanoparticles prepared by a modified sol–gel method, R. Soc. Open Sci., 7, 200708.http://dx.doi.org/10.1098/rsos.200708
[15] Das,S., Srivastava, V.C. (2017). Synthesis and Characterization of ZnO/CuO nanocomposite byelectrochemical method.Materials Science in Semiconductor Processing, 57, 173–177,https://doi.org/10.1016/j.mssp.2016.10.031
[16] Li, H., Zhang, Z., Liu, Z. (2017).Application of artificial neural networks for catalysis: Areview, Catalysts, 7(10),306.https://doi.org/10.3390/catal7100306
[17]Igwegbe, C.A., Mohmmadi, L., Ahmadi, S., Rahdar, A., Khadkhodaiy, D., Dehghani, R., Rahdar, S. (2019). Modeling of Adsorption of Methylene Blue dye on Ho-$CaWO_4$nano-particles using Response Surface Methodology (RSM) and Artificial Neural Network (ANN) techniques. *Journal of MethodsX*, 6, 1779-1797. https://doi.org/10.1016/j.mex.2019.07.016
[18]Elmolla, E.S., Chaudhuri, M., Eltoukhy, M. M.(2010)**.** The useof Artificial Neural Network (ANN) for modeling of COD removal from antibiotic aqueous solution by Fentonprocess, *J. Hazard. Mater.*, 179, 127–134.
[19] Lee, K. M., Lai, C. W., Ngai, K. S., & Juan, J. C.(2016). Recent developments of zinc oxide based photocatalyst in water treatment technology: A review.*Water Research. Elsevier Ltd.*, 88, 428-448. https://doi.org/10.1016/j.watres.2015.09.045
[20] Manalu, J. L., Soegijono, B., Indrani, D. J. (2015). Characterization of Hydroxyapatite Derivedfrom Bovine Bone. *Asian Journal of Applied Sciences*, 03(4), 758-765, www.ajouronline.com.
[21] Taqvi, S.A., Tufa, L.D., Zabiri, H., Mahadzir, S., Maulud, A.S., Uddin,F. (2017). Artificialneural network for anomalies detection in a distillation column, *Asian SimulationConference*, 302–311
[22] Monteagudo, J., Durán, A. (2006). Fresnel lens to concentrate solar energy for the photocatalytic decoloration and mineralization of orange II in aqueous solution,*Chemosphere***,** 65, 1242–1248. https://doi.org/10.1016/j.chemosphere.2006.04.057
[23] Sharifi, S. H., Archin, S.,Asadpour, G. (2018)**.** Optimization of Process Parameters by Response Surface Methodology for Methylene Blue Removal Using Cellulose Dusts, *Civil Engineering Journal***,**4 (3),620-634. https://creativecommons.org/licenses/by/4.0/
[24] Zulfiqar, M., Chowdhury, S., Sufian, S., Omar, A. A. (2018). Enhanced photocatalytic activityof orange II in aqueous solution using solvent based TiO_2 nanotubes: Kinetics, Equilibrium, and thermodynamic studies, *J. Clean. Prod.*, Vol. 203, https://doi.org/10.1016/j.jclepro.2018.08.324
[25] Chowdhury, S., Mandal, P. C., Zulfiqar, M. Subbarao, D. (2016). Development of ionothermalsynthesis of titania nanomaterial for waste-water treatment, Adv. Mat. Res.**,**537–541
[26] Zulfiqar, M., Chowdhury, S., Omar, A. (2018). Hydro-thermal synthesis of multiwalled TiO2 nanotubes and its photocatalytic activities for orange II removal, *Sep. Sci. Technol.*, 53, 1412–1422.https://doi.org/10.1080/01496395.2018.1444050
[27] Elhadj, M., Samira,A., Mohamed,T., Djawad, F., & Asma, A. (2019). Removal of Basic Red46- dye from aqueous solution by adsorption & photocatalysis: equilibrium, isotherms, kinetics, and thermodynamicstudies. Separation Science and Technology,1-17.
https://doi.org/10.1080/01496395.2019.1577896
[28]Sarvani, R., Damani, E., Ahmadi, SH. (2018).Adsorption Isotherm and Kinetics Study: Removal of phenol using adsorption ontomodified Pistaciamuticashells, *Iran. J. Health Sci.*, 6, 33-2.https://doi.org/10.29252/jhs.6.1.33
[29]Miyah, Y., Lahrichi, A., Idrissi, M., Boujraf, S., Taouda, H., Zerrouq, F. (2017).Assessment of Adsorption kinetics for removal potential ofCrystalViolet dye from aqueous solutions using Moroccan-pyrophyllite, J. Assoc. Arab Univ. Basic Appl. Sci., 23, 20–28.
https://doi.org/10.1016/j.jaubas.2016.06.001
[30]Wu, F.C., Tseng, R.L.; Juang, R.S. (2009).Initial behavior of intraparticle diffusion model used in thedescriptionof adsorption kinetics. *ChemicalEngineering Journal*, 153 (1–3):1–8,https://doi.org/10.1016/j.cej.2009.04.042

[31]Ocampo-Perez, R., Leyva-Ramos, R., Mendoza-Barron,J.,Guerrero Coronado,R.M. (2011)Adsorption rate of phenol from aqueous solution onto organo-bentonite: surfacediffusion and kinetic models, *J. Colloid Interface Sci.*, 364, 195–204. https://doi.org/10.1016/j.jcis.2011.08.032.
[32] Yao, C., Chen, T. (2017). A film-diffusion-basedadsorption kinetic equation and its application. *Chemical Engineering Research and Design*, 119:87–92. https://doi.org/10.1016/j.cherd.2017.01.004
[33]Weber Jr. W.J., Morris, J.C.,(1963). J. Sanitary Eng. Div. ASCE, 89 (SA2) 31.
[34]Bhatnagar, A., Kumar, E., Minocha, A. K., Jeon, B-H.,Song, H., &Seo, Y-C.(2009).Removal of Anionic Dyes from Water usingCitrus limonum (Lemon) Peel: Equilibrium Studies and Kinetic Modeling, SeparationScience and Technology, 44(2), 316-334,https://doi.org/10.1080/01496390802437461
[35]Igwegbe, C.A., Onukwuli, O.D., Nwabanne, J.T.(2016)Adsorptive removal of vat yellow 4 on activated *Mucunapruriens*(velvet bean)seed shells carbon, Asian J. Chem. Sci., 1 (1); 1–16. https://doi.org/10.9734/AJOCS/2016/30210.
[37]Hammud, H. H., Chahine, M., El-Hamaoui, B., and Hanifehpour, Y. (2013).Lead uptakeby new silica carbon nanoparticles, European J. Chemistry, 4 (4),432-440. https://doi.org/10.5155/eurjchem.4.4.425-433.776
[38]Ayawei, N., Ekubo, A. T., Wankasi, D. and Dikio, E. D. (2015).“Adsorption of Congo red by Ni/Al-CO_3: equilibrium, thermodynamicand kinetic studies,” *Oriental Journal of Chemistry*, 31(30),1307–1318. http://dx.doi.org/10.13005/ojc/310307
[39]Hutson, N. D. and Yang,R. T. (1997). “Theoretical basis for the DubininRadushkevitch (D-R) adsorption isotherm equation,” *Adsorption*, vol. 3, no. 3, pp. 189–195.https://doi.org/10.1007/BF01650130
[40]Rania, F., and Yousef, N. S.(2015). Equilibrium and Kinetics studies of adsorption of Copper (ii)ions natural biosorbent.*International Journal of Chemical Engineering and Applications*, 6(5), 319-324, https://doi.org/10.7763/IJCEA.2015.V6.503
[41] Wu, F.-C., Liu, B.-L.., Wu, K.-T., and. Tseng, R.-L. (2010)**.** A new linear form analysis of the Redlich-Peterson Isotherm equation for the adsorption of dyes. *Chemical Engineering Journal*, 162(1), 21–27. https://doi.org/10.1016/j.cej.2010.03.006
[42] Widiarti, N., Sae, J.K. and Wahyuni, S. (2017).Synthesis of CuO-ZnO nano-composite and its application as an antibacterial agent. *Materials Science and Engineering*,172**,**012-036,https://doi.org/10.1088/1757-899X/172/1/012036.
[43]Treybal, R. E. (1998). Mass Transfer Operations(McGrew Hill, New York, 10th ed).
[44]Rokhmat,M.,Wibowo, E., Khairurrijal,S.,Abdullaha, M. (2017).Performance Improvement of TiO_2/CuO Solar Cell by Growing CopperParticle using Fix Current Electroplating Method, Engineering Physics International Conference, Procedia Engineering, 170, 72 – 77, https://doi.org/10.1016/j.proeng.2017.03.014
[45] Makeswari, M. and Saraswathi, P. (2020). Photocatalytic degradation of methylene blue and methyl orange from aqueous solution using solar light onto chitosan bi-metal oxide composite. SN Appl.Sci., 2,336.https://doi.org/10.1007/s42452-020-1980-4
[46] Annadurai, G., Rajesh Babu, S., Mahesh, K. P. O. andMurugesan, T. (2000).Adsorption and biodegradation of phenol by chitosan immobilized *Pseudomonasputida* (NICM 2174), Bioprocess Eng., 22, 493-501.https://doi.org/10.1007/s004499900092
[47] Murphy, O. P., Vashistha, M., Palanisamy, P. and Kamar, K. V.(2023).A Reviewon the AdsorptionIsothermsand DesignCalculations for the Optimizationof AdsorbentMassand ContactTime, *ACS Omega*, 8, 17407-17430. https://doi.org/10.1021/acsomega.2c08155